

# The Oligocene–Miocene transition climate recorded in a lacustrine sequence, Ebro Basin: preliminary insights

*El clima de la transición Oligoceno-Mioceno registrado en una secuencia lacustre de la cuenca del Ebro: resultados preliminares*

Concha Arenas<sup>1,2</sup>, Lluís Cabrera<sup>3</sup>, M. Cinta Osácar<sup>1,2\*</sup>, Luis Valero<sup>3</sup>, Javier Pérez-Rivarés<sup>1</sup>, Joaquín Bastida<sup>4</sup>, Miguel Garcés<sup>3</sup>, Luis Auqué<sup>1</sup>, Andrés Gil<sup>1,2</sup> and María J. Gimeno<sup>1</sup>

<sup>1</sup>Department of Earth Sciences, University of Zaragoza, 50009 Zaragoza, Spain

[carenas@unizar.es](mailto:carenas@unizar.es), [cinta@unizar.es](mailto:cinta@unizar.es), [perezrivares@gmail.com](mailto:perezrivares@gmail.com), [lauque@unizar.es](mailto:lauque@unizar.es), [agil@unizar.es](mailto:agil@unizar.es), [mjgimeno@unizar.es](mailto:mjgimeno@unizar.es).

<sup>2</sup>Institute for Research on Environmental Sciences of Aragón (IUCA) and GeoTransfer Group

<sup>3</sup>Department of Earth and Ocean Dynamics, Geomodels Research Institute and Research Group of Geodynamics and Basin Analysis. Universitat de Barcelona

[lluis.cabrera@ub.edu](mailto:lluis.cabrera@ub.edu), [luisvalero@ub.edu](mailto:luisvalero@ub.edu), [mgarces@ub.edu](mailto:mgarces@ub.edu)

<sup>4</sup>Unit of Geology, University of Valencia, Spain

[bastida@uv.es](mailto:bastida@uv.es).

\*Corresponding author

## ABSTRACT

The climate evolution across the Oligocene–Miocene transition has been studied through a 23.5 to 22 Ma succession in the eastern Ebro Basin, dated by magnetostratigraphy. The study is based on the  $\delta^{13}\text{C}$  and  $\delta^{18}\text{O}$  composition coupled with sedimentological analysis of a dominantly lacustrine and palustrine carbonate succession, focusing on the limestone facies. The deposits formed in alluvial plain, saline mud flat, and carbonate lacustrine and palustrine depositional environments. Changes in lake water level and hydrodynamics, and biological processes triggered the formation of distinct carbonate facies, causing isotopic differences among them. The isotopic variations likely reflect changes in the precipitation/evaporation ratio and temperature in the Ebro Basin that might be the regional record of the Mi-1 Glaciation. A change in variability in  $\delta^{13}\text{C}$  and  $\delta^{18}\text{O}$  and an inflection in  $\delta^{13}\text{C}$  mark the Oligocene–Miocene boundary (23.03 Ma). The decrease in  $\delta^{13}\text{C}$  and  $\delta^{18}\text{O}$  variability may correspond to steadier depositional, climatic and hydrological conditions through time.

**Key-words:** Oligocene–Miocene transition, lacustrine and palustrine carbonates, paleoclimate,  $\delta^{13}\text{C}$  and  $\delta^{18}\text{O}$ , NE Iberia.

## RESUMEN

Se estudia la evolución climática de la transición Oligoceno-Mioceno en una sucesión lacustre de la parte oriental de la cuenca del Ebro, de 23,5 a 22 Ma, según la magnetoestratigrafía. Se basa en la composición de  $\delta^{13}\text{C}$  y  $\delta^{18}\text{O}$ , junto con el análisis sedimentológico, de materiales mayoritariamente carbonatados, lacustres y palustres, centrado en las facies de caliza. Los depósitos se formaron en ambientes de llanuras aluviales y fangosas evaporíticas, lacustres y palustres. Los cambios en el nivel de agua del lago y la hidrodinámica, así como los procesos biológicos, ocasionaron la formación de facies carbonatadas distintas e isotópicamente diferentes. Probablemente estas diferencias isotópicas reflejan cambios en la relación precipitación/evaporación y en la temperatura en la cuenca del Ebro, que podrían ser la expresión regional de la Glaciación Mi-1. El límite Oligoceno-Mioceno (23,03 Ma) se manifiesta por un cambio en la variabilidad de  $\delta^{13}\text{C}$  y  $\delta^{18}\text{O}$ , junto con una inflexión en  $\delta^{13}\text{C}$ . La disminución en la variabilidad de  $\delta^{13}\text{C}$  y  $\delta^{18}\text{O}$  puede corresponder a una tendencia hacia condiciones de depósito, climáticas e hidrológicas más estables.

**Palabras clave:** Transición Oligoceno-Mioceno, carbonatos lacustres y palustres, paleoclima,  $\delta^{13}\text{C}$  y  $\delta^{18}\text{O}$ , NE Iberia.

Geogaceta, 75 (2024), 11–14

<https://doi.org/10.55407/geogaceta100684>

ISSN (versión impresa): 0213-683X

ISSN (Internet): 2173-6545

Fecha de recepción: 30/06/2023

Fecha de revisión: 24/10/2023

Fecha de aceptación: 24/11/2023

## Introducción

Alternating warming and cooling conditions have been extensively recorded through the Oligocene–Miocene Transition (OMT). A warming interval at the latest Oligocene characterised the OMT beginning ( $\approx 24.8$  Ma), then followed by cooling conditions related to an Antarctic ice-sheet expansion (Mi-1 Glaciation; Zachos *et al.*, 2001). The Oligocene–Miocene boundary (OMB), set at 23.03 Ma, coincides with this cooling process, which caused varied effects on oceans and continents, although large-scale decreases in temperature and

precipitation have usually been proposed. The characteristics of the OMT climate have not been described in detail in the continental realm mainly due to the lack of accurately dated records, which indeed are suitable for searching and applying indicators relevant to climate. This contribution aims to show the preliminary characterisation of the OMT climate in NE Iberia, based on the C and O stable isotope composition coupled with sedimentological analysis of a well-exposed lacustrine and palustrine carbonate succession in the eastern Ebro Basin. The approach is focused on the limestone facies. The succession has been

dated through robust magnetostratigraphy and cyclostratigraphy (Valero *et al.*, 2014).

## Geological setting

The study area is located in the eastern central part of the Ebro Basin (Fig. 1), close to the Mequinenza village. The outcropping rocks in the study area belong to the genetic stratigraphic unit T4 (late Oligocene to Early Miocene; Muñoz *et al.*, 2002). This unit includes coarse-to fine-grained alluvial detrital deposits sourced from the three basin margins,

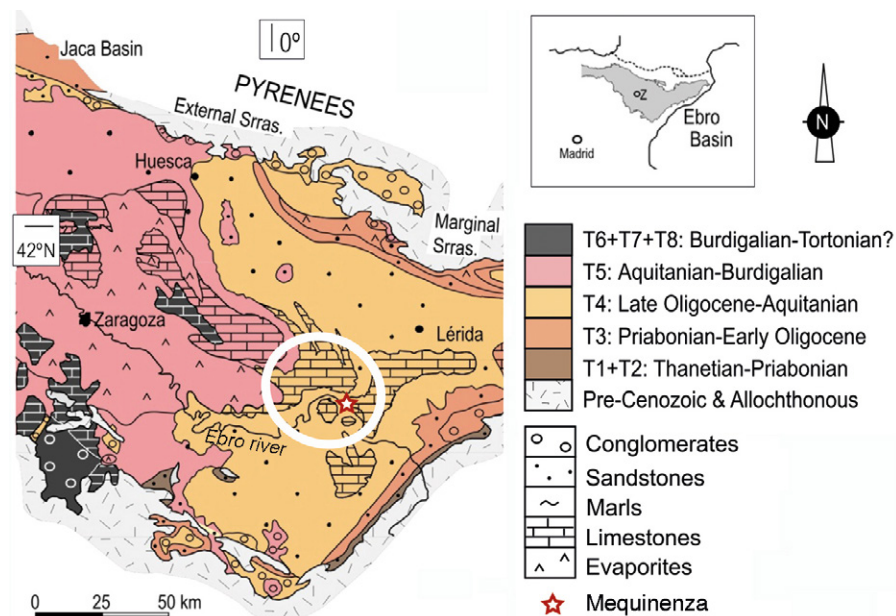


**Fig. 1.- Location of the study area (white circle) in the Ebro Basin. T1 to T8: Stratigraphic genetic units after Muñoz et al. (2002). See color figure in the web.**

*Fig. 1.- Localización del área estudiada (círculo blanco) en la Cuenca del Ebro. T1 a T8: unidades estratigráficas genéticas según Muñoz et al. (2002). Ver figura en color en la web.*

lacustrine evaporite deposits in the basin centre and west, and lacustrine carbonate deposits in the basin east sector (Pardo *et al.*, 2004). The magnetostratigraphic studies allowed the accurate dating of the Oligocene to Early Miocene record in these formations, and have shown that the Oligocene–Miocene boundary occurs within the study carbonate succession (Mequinenza section; Barberà *et al.*, 2001; Valero *et al.*, 2014).

**Methods and materials**

A 104 m-thick succession, spanning from 23.5 to 22 Ma, was measured and sampled for mineralogical, sedimentological and stable isotope analyses. Base and top coordinates are, respec-

tively: 41.390483° N / 0.297650° E and 41.394400° N / 0.297750° E.

The δ<sup>13</sup>C and δ<sup>18</sup>O analyses were performed on 0.2-0.5 mg of calcite micrite of limestones (N=86), picked with a microdrill under magnification, avoiding cements. None of the samples contained significant amounts of dolomite to affect the isotopic results.

The analyses followed the usual procedures at the *Centros Científicos y Tecnológicos* of the Universitat de Barcelona (see Osácar *et al.*, 2013 for details). In order to avoid the interference of diverse factors in the isotopic evolution through time, only limestone facies have been considered herein. The ages (e.g., the OMB) were determined by interpolation within each magnetic polarity chron.

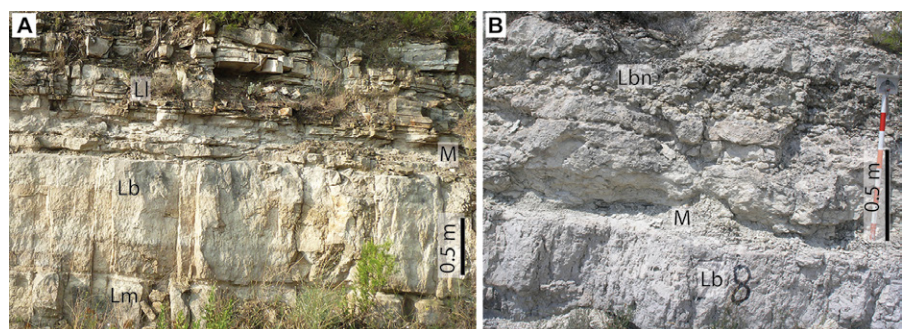


**Fig. 2.- Field views of sedimentary facies in the study area. A) Bioclastic massive and bioturbated limestones (Lm and Lb), marls (M) and laminated limestones (LI). B) Bioclastic bioturbated (Lb), with vertical root traces, nodular limestones (Lbn) and marls (M). See color figure in the web.**

*Fig. 2.- Imágenes de campo de facies sedimentarias en el área estudiada. A) Calizas bioclásticas masivas y bioturbadas (Lm y Lb), margas (M) y calizas laminadas (Lm). B) Calizas bioturbadas (Lb) con trazas verticales de raíces, calizas nodulosas (Lbn) y margas (M). Ver figura en color en la web.*

**Stratigraphy and sedimentology**

The studied section consists of grey to beige limestones, grey and green marls, orange to red and brown mudstones and light brown sandstones. Limestones are volumetrically the most abundant lithology. Marls appear as interbeds between limestone strata. Mudstones and sandstones occur at the base of the section, along with gypsum. The latter occurs as microcrystalline nodules and cements, as well as fibrous gypsum filling voids, commonly cracks. The sandstones are fine- to coarse-grained litharenites that constitute both tabular and lenticular bodies, either structureless or with through-cross stratification.

The main limestone facies, consisting of mainly calcite, are distinguished based on textural and structural features:

Massive limestones (Lm) are charophyte, gastropod and ostracod mudstones, wackestones and packstones. These limestones form tabular, lenticular and irregularly-shaped strata, centimeter to 1 meter-thick, which can be either structureless or less commonly have horizontal lamination or banding (Figs. 2A and 3A). Gentle root traces are present at places.

Laminated limestones (LI) consist of ostracod and charophyte mudstones and wackestones, in some cases with gastropod fragments and intraclasts. The long axes of bioclasts may appear parallel to the depositional surface. Scattered detrital silt- to sand-size quartz grains are present in some cases. Variable amount and type of these components produces lamination. These limestones constitute tabular and lenticular strata, centimeter to decimeter thick, showing horizontal and ripple lamination, cross stratification and, at places, hummocky-cross stratification (Figs. 2A, 3B and 3C).

Bioturbated and nodulised limestones (Lb and Lbn) are charophyte, gastropod and ostracod mudstones and wackestones containing vertical root traces (facies Lb), and nodules and breccia (facies Lbn). Both Lb and Lbn include desiccation features, e.g., typical circum-granular cracks. Facies Lb form tabular and lenticular strata up to 1 m thick, which may show compensating morphologies. Facies Lbn constitute tabular and more frequently irregularly shaped strata, centimeter to decimeter thick, with diffuse bases and tops (Figs. 2B and 3D).



## $\delta^{13}\text{C}$ and $\delta^{18}\text{O}$ composition

Both the global average  $\delta^{13}\text{C}$  values and facies  $\delta^{13}\text{C}$  values are lower for the Miocene than the Oligocene. Facies LI display the highest average values (Table I; Fig. 4). The global average  $\delta^{18}\text{O}$  values are similar for the Miocene and Oligocene. Facies LI show lower values than the rest of facies. The variability is smaller for  $\delta^{18}\text{O}$  than for  $\delta^{13}\text{C}$ , and is wider in the Oligocene than in the Miocene, except for the  $\delta^{13}\text{C}$  LI values. The correlation between  $\delta^{13}\text{C}$  and  $\delta^{18}\text{O}$  is poorly significant ( $r=-0.32$ ).

The  $\delta^{13}\text{C}$  values distinctly decrease through time, whereas the  $\delta^{18}\text{O}$  values do not show a clear tendency (Fig. 5). The Oligocene record shows a significantly wide  $\delta^{13}\text{C}$  and  $\delta^{18}\text{O}$  variability that sharply decreases right after the OMB; the rather steady evolution includes periods of some  $\delta^{13}\text{C}$  and  $\delta^{18}\text{O}$  variability. A change in the  $\delta^{13}\text{C}$  trend occurs around the OMB, from increasing in the Oligocene to decreasing in the Miocene. A subtle decreasing–increasing inflection is recorded by the Miocene  $\delta^{18}\text{O}$  values at  $\approx 22.6$  Ma.

## Discussion

The textural and structural characteristics of the studied rocks allow interpreting their formation in three main depositional environments (e.g. as described by Cabrera *et al.*, 1985; Platt, 1989; Luzón, 1994; Arenas and Pardo, 1999; Alonso-Zarza, 2003):

- Distal alluvial plain with fluvial channels and saline mud flat (mudstones and sandstones with gypsum interbeds and disperse nodules). These conditions occurred at the base of the studied section (late Oligocene).

- Carbonate lacustrine environment, with two distinct depositional settings:

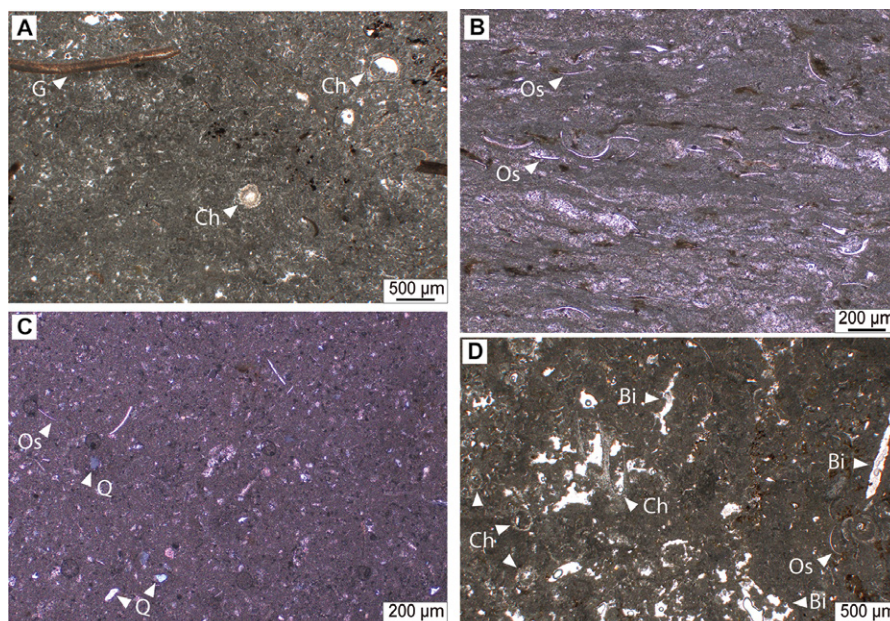


**Fig. 3.- Photomicrographs taken in optical microscope (parallel-polarised light). A) Bioclastic massive limestone (Lm). B) Laminated limestone (LI). Ostracod and gastropod shells oriented parallel to deposition surface. C) Detail of laminated limestones containing detrital quartz grains. D) Bioclastic bioturbated limestone (Lb). Pores reflect root traces (Bi). G: gastropod shell; Ch: charophyte gyrogonite and thalli; Os: ostracod shells; Q: quartz grains. See color figure in the web.**

*Fig. 3.- Microfotografías tomadas en microscopio óptico (luz polarizada paralela). A) Calizas bioclásticas masivas (Lm). B) Calizas laminadas (LI). Conchas de ostrácodos y gasterópodos orientadas paralelamente a la superficie de depósito. C) Detalle de calizas laminadas que contienen granos detríticos de cuarzo. D) Calizas bioclásticas bioturbadas (Lb). Las cavidades corresponden a trazas de raíces (Bi). G: concha de gasterópodo; Ch: girogonitos y tallos de carofitas; Os: conchas de ostrácodos; Q: granos de cuarzo. Ver figura en color en la web.*

1. shallow lake inhabited by ostracods, gastropods and charophytes, with quiet lime mud deposition (facies Lm), and

2. shallow to slightly deep lake, with varying biota content and fine detrital inputs, affected by surge producing low to high energy structures (facies LI).

Both settings represent changes in lake level and hydrodynamic conditions through time.

- Carbonate palustrine environment, either formed of a vegetated fringe affected by lake level variations during short time periods (facies Lb) or consisting of

extensive fringes affected by long and/or repetitive exposure periods (facies Lbn) causing calcrete development. Both settings represent lake level changes of different reach through time that predominated in the middle part of the studied Miocene succession.

Marls are interpreted as formed in offshore lake areas in relation to settling of fine-sediment through fluvial supply.

The  $\delta^{13}\text{C}$  and  $\delta^{18}\text{O}$  values are typical of fresh water bodies that had moderate to high soil- or plant-derived  $\text{CO}_2$  inputs (Arenas *et al.*, 1997; Leng and Marshall, 2004).

The isotopic differences among the limestone facies respond to the variable intensity and/or frequency of water renewal and to the biological processes occurring in and around the lake, coinciding with or modulated by specific climatic and hydrodynamic conditions. The low  $\delta^{13}\text{C}$  values of Lb+Lbn are linked to the intense biological activity. The low  $\delta^{18}\text{O}$  values of both Oligocene and Miocene LI facies are related to a higher water renewal respect to the other facies; two samples with extreme values would represent more intense  $^{16}\text{O}$  supply.

The isotopic trends across the OMT (Fig. 5) likely reflect changes in the pre-

Facies	N Olig-N Mioc	$\delta^{13}\text{C}$ Olig	$\delta^{13}\text{C}$ Mioc	$\delta^{18}\text{O}$ Olig	$\delta^{18}\text{O}$ Mioc
		$\bar{x}$ (s)	$\bar{x}$ (s)	$\bar{x}$ (s)	$\bar{x}$ (s)
Lm	12 - 28	-5.40 (1.29)	-5.68 (1.02)	-6.19 (0.47)	-6.08 (0.34)
LI	7 - 7	-4.02 (0.66)	-5.55 (1.20)	-7.25 (1.22)	-6.77 (0.75)
Lb+Lbn	5 - 27	-5.50 (1.28)	-6.32 (0.73)	-5.99 (0.72)	-6.51 (0.43)
Total	24-62	-5.02 (1.30)	-5.95 (0.97)	-6.46 (0.94)	-6.35 (0.50)

**Table I.- Average ( $\bar{x}$ ) and standard deviation (s) of  $\delta^{13}\text{C}$  and  $\delta^{18}\text{O}$  of the analysed limestones, by facies and as a whole (Total), for Oligocene (Olig) and Miocene (Mioc). N: number of analyses. Lm: massive limestones; LI: laminated limestones; Lb+Lbn: bioturbated and nodulised limestones.**

*Tabla I.- Media ( $\bar{x}$ ) y desviación típica (s) de  $\delta^{13}\text{C}$  y  $\delta^{18}\text{O}$  de las calizas analizadas, por facies y en total (Total), para Oligoceno (Olig) y Mioceno (Mioc). N: número de análisis. Lm: calizas masivas; LI: calizas laminadas; Lb+Lbn: calizas bioturbadas y nodulosas.*

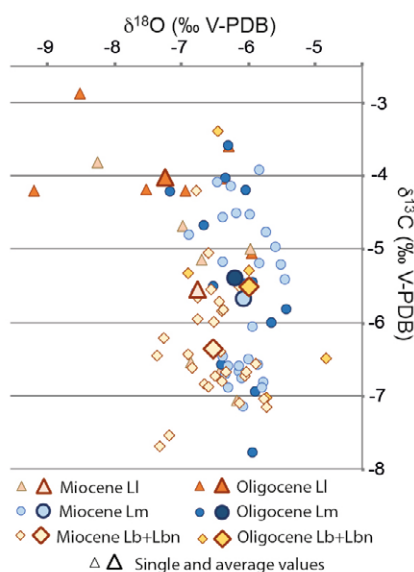


**Fig. 4.-  $\delta^{13}\text{C}$  and  $\delta^{18}\text{O}$  values of the studied limestone facies. See color figure in the web.**

Fig. 4.- Valores de  $\delta^{13}\text{C}$  y  $\delta^{18}\text{O}$  de las facies de calizas estudiadas. Ver figura en color en la web.

precipitation/evaporation ratio and temperature in the Ebro Basin that might be the regional response to the global Mi-1 Glaciation (Zachos *et al.*, 2001). In this context, the isotopic differences between the Oligocene and Miocene facies can be linked to these changes. The diminishing  $\delta^{13}\text{C}$  and  $\delta^{18}\text{O}$  variability may reflect an evolution towards steadier depositional, climatic and hydrological conditions.

**Conclusions**

The 23.5 to 22 Ma studied deposits in the eastern Ebro Basin formed in alluvial plain, saline mud flat, carbonate lacustrine and carbonate palustrine environ-

ments. Changes in lake water level and hydrodynamics triggered the formation of the distinct carbonate facies.

The different  $\delta^{13}\text{C}$  and  $\delta^{18}\text{O}$  values of the diverse facies are consistent with variations in the depositional and climatic parameters, e.g., via lake-level changes.

Despite the isotopic composition differences among the facies, owing to the lake-level changes and hydrodynamic conditions, the limestone facies reflect consistent isotopic trends through time, e.g. an inflection around the OMB and subtle changes through the studied Miocene section, which would represent overall varying climatic conditions across the OMT.

**Authors contribution**

The authors have participated in the field work, laboratory tasks and subsequent analysis of the results, as well as in the manuscript preparation.

**Acknowledgements**

Grants PID2019-106440GB-C21 and PID2019-106440GB-C22 funded by MCIN/AEI/10.13039/501100011033; Research Groups Geodynamics and Basin Analysis (2021-SGR00076), Universitat de Barcelona, and GeoTransfer Group of the Aragón Government-University of Zaragoza.

**References**

Alonso-Zarza, A.M. (2003). *Earth-Science Reviews* 60, 261–298. <https://doi.org/dnz3bh>  
 Arenas, C. y Pardo, G. (1999). *Palaeogeography, Palaeoclimatology, Palaeoecology* 151, 127–148.

<https://doi.org/dpzrnc>  
 Arenas, C., Casanova, J. y Pardo, G. (1997). *Palaeogeography* 128, 133–155. <https://doi.org/dbxvsp>  
 Barberà, X., Cabrera, L., Marzo, M., Parés, J.M. y Agustí, J. (2001). *Planetary Science Letters* 187, 1–16. <https://doi.org/d2ngvb>  
 Cabrera, L., Colombo, F. y Robles, S. (1985). *6th European Reg.Meeting IAS. Exc. Guidebook*, 10, 393–492.  
 Leng, M.J. y Marshall, J.D. (2004). *Quaternary Science Reviews* 23, 811–831. <https://doi.org/fkk55c>  
 Luzón, A. (1994). *Los materiales del tránsito Oligoceno-Mioceno del sector centro-oriental de la Depresión del Ebro. Análisis estratigráfico e interpretación evolutiva*. Degree Thesis Univ. of Zaragoza, 259 pp.  
 Muñoz, A., Arenas, C., González, A., Luzón, A., Pardo, G., Pérez, A. y Villena, J. (2002). In: *The Geology of Spain* (Gibbons, W. and Moreno, T. Eds.). The Geological Society, London, 301–309.  
 Osácar, M.C., Arenas, C., Vázquez-Úrbez, M., Sancho, C., Auqué, L.F. y Pardo, G. (2013). *Journal of Sedimentary Research* 83 (4), 309–322. <https://doi.org/kw6f>  
 Pardo, G., Arenas, C., González, A., Luzón, A., Muñoz, A., Pérez, A., Pérez-Rivarés, F.J., Vázquez-Úrbez, M. y Villena, J. (2004). En: *Geología de España* (Vera, J.A. Ed.). SGE- IGME, Madrid, 533–543.  
 Platt, N.H. (1989). *Sedimentology* 36, 665–684. <https://doi.org/dk8jcf>  
 Valero, L., Garcés, M., Cabrera, L., Costa, E., y Sáez, A. (2014). *Earth and Planetary Science Letters* 408, 183–193. <https://doi.org/f6vmq4>  
 Zachos, J., Pagani, M., Sloan, L., Thomas, E. y Billups, K. (2001). *Science* 292, 686–693. <https://doi.org/ckdj6v>

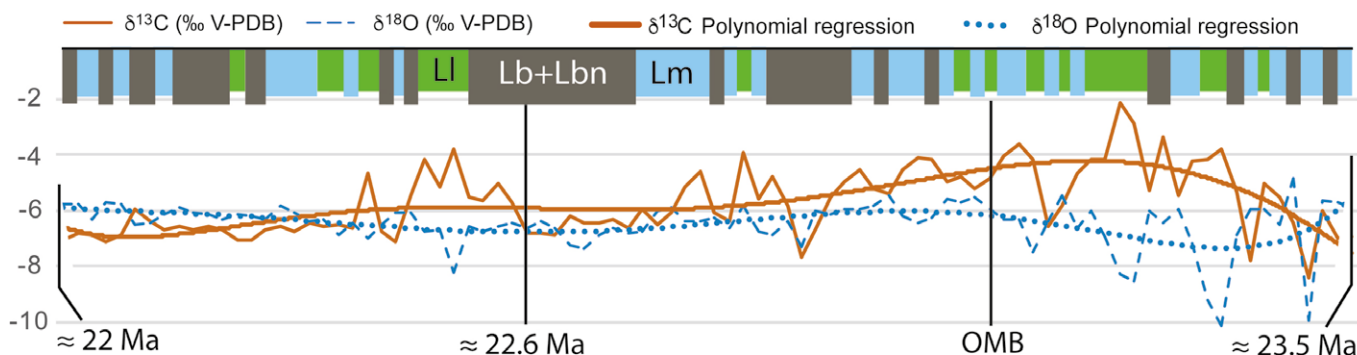


**Fig. 5.-  $\delta^{13}\text{C}$  and  $\delta^{18}\text{O}$  values of the analysed limestones through time. The jagged lines correspond to the plotted data. The tendency lines correspond to polynomial regressions of degree 6. See color figure in the web. Dominant facies are represented above; symbols like in Stratigraphy and sedimentology section.**

Fig. 5.- Evolución temporal de  $\delta^{13}\text{C}$  y  $\delta^{18}\text{O}$  de las calizas analizadas. Las líneas dentadas corresponden a los datos representados. Las líneas de tendencia corresponden a regresiones polinómicas de grado 6. Ver figura en color en la web. Las facies dominantes aparecen en la parte superior; las siglas como en la sección de Stratigraphy and sedimentology.